

Small-scale convection in the D'' layer

V. S. Solomatov

Department of Physics, New Mexico State University, Las Cruces, New Mexico, USA

L.-N. Moresi

Australian Geodynamics Cooperative Research Centre, CSIRO Exploration and Mining, Nedlands, Western Australia, Australia

Received 17 November 2000; revised 17 June 2001; accepted 22 June 2001; published 22 January 2002.

[1] Small-scale convection has been suggested as a possible explanation for seismic heterogeneities in the D'' layer of the Earth's mantle. Recently developed scaling laws for convection with realistic viscosities allow quantitative assessment of this hypothesis. Large temperature and viscosity contrasts across the thermal boundary layer at the core-mantle boundary suggest that small-scale convection starts at the bottom of the thermal boundary layer and propagates upward before the thermal boundary layer as a whole becomes unstable. The convection boundary is likely to become a chemical boundary as a result of mixing within the convective layer. This implies that the D'' discontinuity can represent both convective and chemical boundary and that the presence or absence of small-scale convection can be responsible for the observed intermittent nature of the D'' discontinuity. Most lateral heterogeneities in the D'' layer are concentrated near the convection boundary, consistent with seismic data. The length scale of lateral temperature variations, the topography of the core-mantle boundary, and the viscosity of the D'' layer are in agreement with observational constraints. The thickness of the secondary thermal boundary layer formed at the bottom of the convective layer is similar to the thickness of the ultralow-velocity zone. The magnitude of lateral variations in temperature can only marginally be responsible for lateral variations in seismic velocities. Variations in the topography of the convection boundary and chemical heterogeneities are likely to be more important factors. A large seismic velocity drop in the ultralow-velocity zone cannot be explained by thermal effects alone and must be caused by other factors such as partial melting. *INDEX TERMS:* 8121 Tectonophysics: Dynamics, convection currents and mantle plumes, 8130 Tectonophysics: Heat generation and transport, 8162 Tectonophysics: Rheology—mantle; *KEYWORDS:* core-mantle boundary, plumes, small-scale convection

1. Introduction

[2] Seismic studies show that the base of the Earth's mantle (the D'' layer) has a complex structure [Young and Lay, 1987; Loper and Lay, 1995; Lay et al., 1998a; Wysession et al., 1998; Garnero, 2000]. The upper boundary of the D'' layer is usually modeled as a discontinuity characterized by 1.5–3% increase in shear velocities. Lateral heterogeneities in the D'' layer are present on scales as small as 100–300 km. These are associated either with topography of the D'' discontinuity or lateral variations in seismic velocities in the D'' layer [Weber, 1993; Lay et al., 1997; Liu et al., 1998]. Anisotropy has also been established in many regions of the D'' layer [Lay et al., 1998b; Kendall and Silver, 1996; Matzel et al., 1996; Garnero and Lay, 1997]. This is in a drastic contrast with the mantle above it, which is isotropic [Meade et al., 1995] and is characterized by heterogeneities of much larger scale and smaller amplitude, most likely associated with the subducting plates [Grand, 1994; Grand et al., 1997; van der Hilst et al., 1997].

[3] Explanations of such a complex structure of the D'' layer usually involve some kind of convection. A compositionally dense layer can develop convective instabilities and form a separate convective system [Montague and Kellogg, 2000]. On the other hand, small-scale convection can also occur because of

large viscosity contrasts. The fact that viscosity variations can play an important role in the dynamics of the thermal boundary layer was realized in early studies of the D'' layer [Loper and Stacey, 1983]. In particular, it was noticed that when the viscosity contrasts reach values as high as 10^3 – 10^4 , convective instabilities occur first in the thermal boundary layer before the thermal boundary layer as a whole becomes unstable [Yuen and Peltier, 1980; Christensen, 1984; Olson et al., 1987; Thompson and Tackley, 1998]. A large, on the order of 1000–2000 K, temperature contrast across the D'' layer [Williams, 1998; Boehler, 2000], an extreme sensitivity of the viscosity to temperature variations in the lower mantle [Karato and Li, 1992; Li et al., 1996; Wang et al., 1999; Ita and Cohen, 1998; Yamazaki and Karato, 2001], and the distribution of hot spots [Ribe and de Valpine, 1994] indicate that the viscosity contrast in the D'' layer can be even higher. At such viscosity contrasts, small-scale convection occurs in the stagnant lid convection regime [Solomatov, 1995].

[4] The goal of this paper is to provide quantitative constraints on small-scale convection in the D'' layer using recently developed scaling laws for stagnant lid convection [Solomatov and Moresi, 2000]. The first part of this study describes the results of numerical simulations with the parameters relevant to the D'' layer. These results agree very well with the scaling relationships for stagnant lid convection. Then we use these relationships to estimate various parameters of small-scale convection in a broader parameter range and compare our estimates with the observed properties of the D'' layer.

2. Model

[5] We use an idealized model similar to that for a conductive thermal boundary layer. Because of the large scale of the Earth's mantle compared to the thickness of the thermal boundary layer, the mantle can be treated as a half-space which initially has a constant uniform temperature T_m . At time $t = 0$ the temperature of the lower boundary is suddenly increased by $\Delta T_{\text{cmb}} = T_c - T_m$, where T_c is the temperature of the core-mantle boundary (CMB). This simple initial condition represents a variety of situations. It can be a moment (1) after the thermal boundary layer nearly has nearly disappeared as a result of plume formation and starts growing again (a typical situation for time-dependent convection); (2) after the thermal boundary layer has been swept away by a large-scale convective flow (also typical for convection); (3) after a subducted slab has reached the bottom of the mantle and starts moving along the core-mantle boundary (a variation of the previous situation and very similar to cooling and convective instabilities of the oceanic lithosphere [Davaille and Jaupart, 1994]); and (4) after core formation 4.5 Gyr ago.

[6] Since the geometry does not have any characteristic length, the equations of thermal convection are convenient to nondimensionalize using $l_0 = [(\kappa\eta_c)/(\alpha\rho g\Delta T_{\text{cmb}})]^{1/3}$ for the length scale, $t_0 = l_0^2/\kappa$ for the timescale, $u_0 = l_0/t_0$ for the velocity scale, and ΔT_{cmb} for the temperature scale, where α is the thermal expansion, g is the acceleration due to gravity, $\kappa = k/\rho c_p$ is the coefficient of thermal diffusion, ρ is the density, k is the thermal conductivity, c_p is the isobaric heat capacity, and η_c is the viscosity at $T = T_c$.

[7] Nondimensional equations of thermal convection with Boussinesq approximation become

$$-\frac{\partial \tau_{ij}}{\partial x_j} + \frac{\partial p}{\partial x_i} = \lambda_i T, \quad (1)$$

$$\frac{\partial u_i}{\partial x_i} = 0, \quad (2)$$

$$\frac{\partial T}{\partial t} + u_i \frac{\partial T}{\partial x_i} = \frac{\partial^2 T}{\partial x_j^2}, \quad (3)$$

where x_i are the coordinates, u_i is the velocity, p and T are the pressure and temperature perturbations, λ_i is a unit vector in the direction of gravity,

$$\tau_{ij} = \eta \left(\frac{\partial u_i}{\partial x_j} + \frac{\partial u_j}{\partial x_i} \right) \quad (4)$$

is the deviatoric stress tensor, and η is the viscosity. The nondimensional initial temperature is $T = 0$ and the bottom temperature is $T = 1$. The bottom boundary is free slip. In particular, this means that any lateral motion of the layer along the core-mantle boundary does not affect the solution.

3. Viscosity

[8] The only nondimensional parameters which control convection are those associated with the viscosity function (the Rayleigh number, which usually appears in convection equations, is absent). The viscosity law is an Arrhenius function of temperature:

$$\eta = b \exp \left(\frac{Q}{RT} \right), \quad (5)$$

where R is the gas constant, Q is the activation enthalpy, and b is a numerical constant. Since the height of convective region is very

Msmall, we neglect the variation of the viscosity with pressure inside the D'' layer, but the value of Q must be calculated at pressures corresponding to the D'' layer.

[9] Uncertainties in Q are high because of poor constraints on composition, mineralogy, oxygen fugacity, and activation volume. The activation enthalpy at the bottom of the mantle can probably be as low as 500 kJ mol⁻¹ and as high as 1500 kJ mol⁻¹ [Karato and Li, 1992; Li et al., 1996; Ita and Cohen, 1998; Wang et al., 1998; Yamazaki and Karato, 2001]. In the numerical simulations we assume $Q = 1500$ kJ mol⁻¹ and consider a wider range later. Also assuming that the temperature at the bottom of the mantle is $T_m = 2900$ K and that the temperature at the CMB is $T_c = 3900$ K [Williams, 1998; Boehler, 2000], the nondimensional viscosity is

$$\eta = \exp \left(\frac{A}{T + T_0} - \frac{A}{T_0} \right), \quad (6)$$

where $A = QR^{-1}(T_c - T_m)^{-1} = 180.5$ and $T_0 = T_m(T_c - T_m)^{-1} = 2.9$. The total viscosity contrast between $T = 0$ and $T = 1$ is 8.5×10^6 .

[10] The problem is fully described with the help of two nondimensional parameters, A and T_0 . However, at such high-viscosity contrasts, convection is confined to a layer at the bottom boundary, where the viscosity varies within a factor of 10 or so and the problem has effectively only one parameter (Frank-Kamenetskii parameter):

$$\theta = \gamma \Delta T_{\text{cmb}}, \quad (7)$$

where

$$\gamma = \frac{Q}{RT_c^2}. \quad (8)$$

For the parameters given above, $\theta \approx 12$.

4. Numerical Simulations

[11] The numerical simulations were performed on 128×128 mesh using finite element code CITCOM. The time of the simulations was limited by the criterion that the numerical domain can be considered as effectively half-space. This means that the thermal perturbations should not reach the upper boundary and that the aspect ratio of the convective layer should be large (perhaps >2 [Solomatov and Moresi, 2000]). Figures 1 and 2 show that after a short period of conductive cooling, the thermal boundary layer becomes unstable and small-scale convection develops in its lower part.

5. Scaling

5.1. Thermal Boundary Layers

[12] The convective region has two secondary thermal boundary layers (Figure 3a). The temperature drop in these boundary layers is controlled by the rheological temperature scale θ^{-1} . The temperature drop in the upper boundary layer is

$$\Delta T_u = T_i - T_L \approx 2.6\theta^{-1}, \quad (9)$$

where T_L is the temperature at the boundary of the convective region (defined according to Solomatov and Moresi [2000]) and T_i is the temperature of the convective region (Figure 2). The temperature drop in the lower boundary layer is

$$\Delta T_l = T_c - T_i \approx 1.1\theta^{-1}. \quad (10)$$

These numbers are in good agreement with the general scaling laws for convection with large viscosity contrasts which suggest

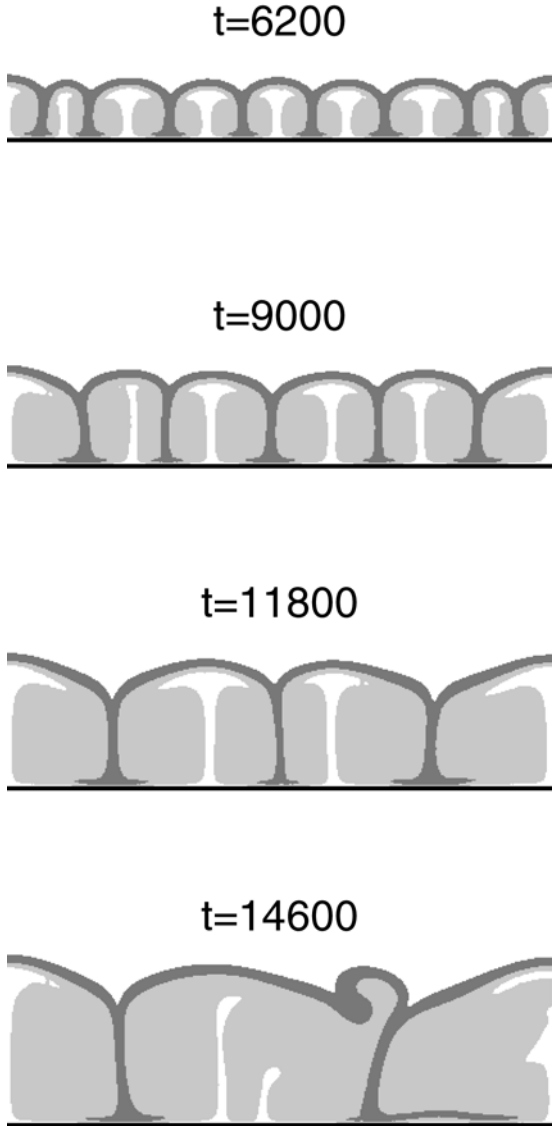


Figure 1. Small-scale convection in the thermal boundary at the CMB is shown at four different nondimensional times: $t = 6200, 9000, 11,800,$ and $14,600$.

$\theta\Delta T_u \approx 2.2-2.6$ and $\theta\Delta T_l \approx 1.1-1.3$ [Davaile and Jaupart, 1993; Manga *et al.*, 2001; Grasset and Parmentier, 1998; Trompert and Hansen, 1998; Dumoulin *et al.*, 1999; Solomatov and Moresi, 2000].

5.2. Lateral Temperature Variations

[13] Lateral temperature variations are localized mainly near the convection boundary (Figure 3b). The amplitude of lateral temperature variations grows with time and stabilizes around $1.9\theta^{-1}$ when convection becomes strongly chaotic (Figure 4a).

5.3. Topography of the Convection Boundary

[14] The localization of temperature variations near the convection boundary seems to be due to large variations in the topography of the convection boundary (Figure 5). Although the scaling laws controlling these variations are difficult to constrain [Fowler, 1985], they scale reasonably well with the average thickness of the convective layer (Figure 4b): $\Delta d \approx 0.08d$.

5.4. Heat Flux

[15] After the onset of convection the heat flux remains approximately constant (Figure 2a). As a result, the growth rate d of the thermal boundary layer also remains approximately constant (Figure 2b). With nondimensional parameters chosen, the heat flux scales as

$$F = 0.5\theta^{-4/3}, \quad (11)$$

where the coefficient is estimated from our simulations and is in agreement with 0.5–0.6 reported for stagnant lid convection. Short intervals of highly variable heat flux are caused by the changes in the number of convective cells: the growth of the convective layer makes the convective cells unstable, and they occasionally have to merge together to form bigger and more stable cells (Figure 1). Convection eventually becomes chaotic as indicated by fluctuations at the end of our simulations. We should also note that it is more appropriate to define θ and the reference viscosity at $T = T_i$; however, the difference between T_i and T_c is not essential.

5.5. Conductive Region

[16] A conductive region is developed on top of the growing convecting layer (Figure 3a). The temperature profile in this region can be found by solving the thermal diffusion equation with the moving boundary. In this case, the moving boundary is the boundary of the convective region where $T = T_L$:

$$T = T_L \exp[-\dot{d}(z - \dot{d}t)], \quad T < T_L, \quad (12)$$

where

$$\dot{d} = \frac{F}{T_i} \quad (13)$$

is the velocity of the moving boundary (derived from the conservation of energy). The effective width of the conductive

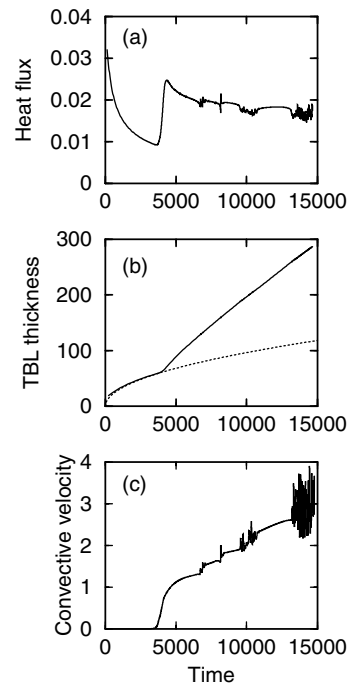


Figure 2. (a) The heat flux at the CMB, (b) the thickness of the thermal boundary layer (the dashed line shows the conductive regime), and (c) the flow velocity in the convective region are shown as functions of time. All parameters are nondimensional.

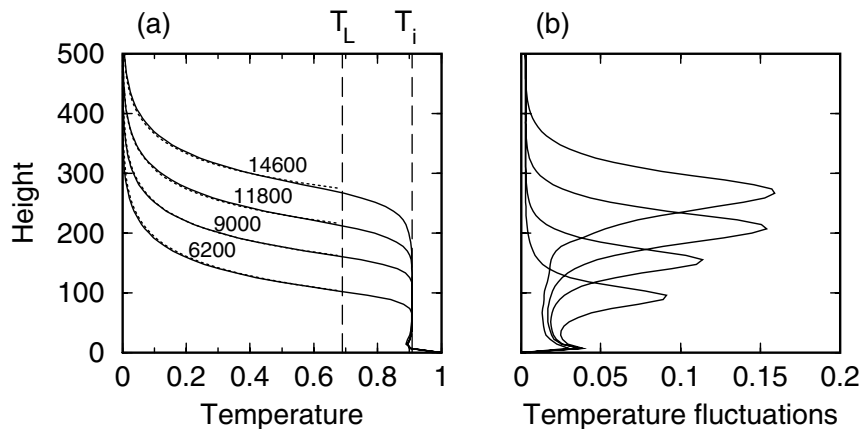


Figure 3. (a) The temperature profiles corresponding to the four snapshots in Figure 1. The temperature T_L of the bottom of the conductive region and the temperature T_i of the convective region are shown with dashed lines. The dotted line is the exponential temperature distribution in the conductive region ($T < T_L$) predicted by equation (12). (b) RMS lateral temperature variation as a function of height.

region can be defined as the height at which the temperature drops to 10% of T_L :

$$\delta_L = 2.3\dot{d}^{-1} = 2.3\frac{T_i}{F} = 2.3\frac{1 - 1.1\theta^{-1}}{F}. \quad (14)$$

The theoretical temperature profiles described by (12) with $\dot{d} \approx 0.02$ determined from Figure 2b show a good fit to the numerical profiles in the conductive region (Figure 3a).

5.6. Convective Velocity

[17] The flow velocity in the convective region increases linearly with time (Figure 2c), which is in agreement with the scaling theory:

$$u = 0.054d\theta^{-2/3} = 0.054\dot{d}t\theta^{-2/3}, \quad (15)$$

where $d = \dot{d}t$ is the thickness of the convective region. The coefficient is similar to 0.053 for internally heated convection

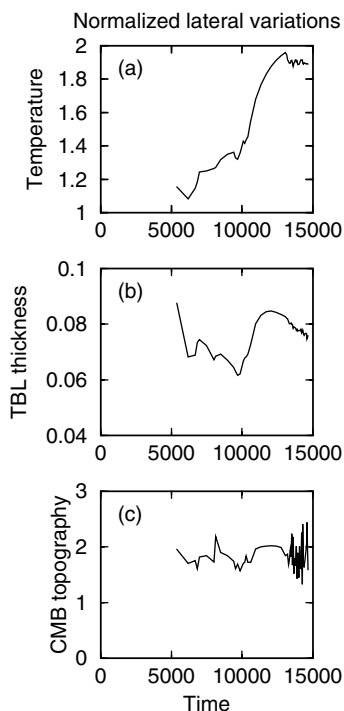


Figure 4. Evolution of (a) RMS lateral temperature variations normalized by θ^{-1} , (b) RMS topography of the convection boundary normalized by the average thickness of the convective layer, and (c) RMS CMB topography normalized by $\alpha T_i \delta_i$.

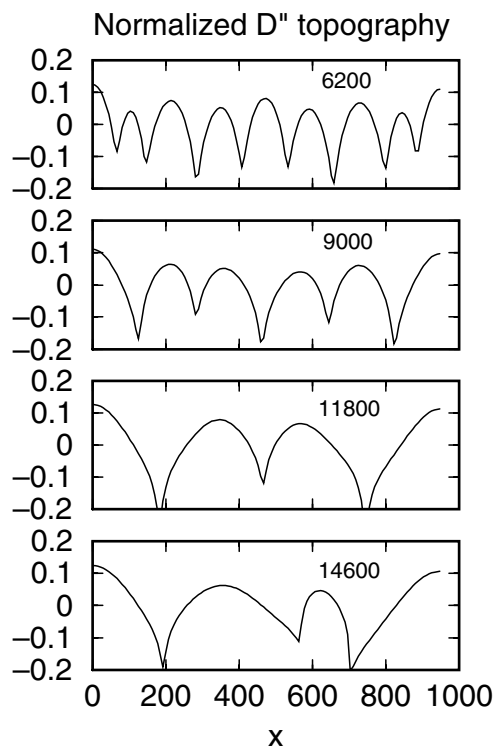


Figure 5. Topography of the convection layer normalized by the average thickness of the convective layer.

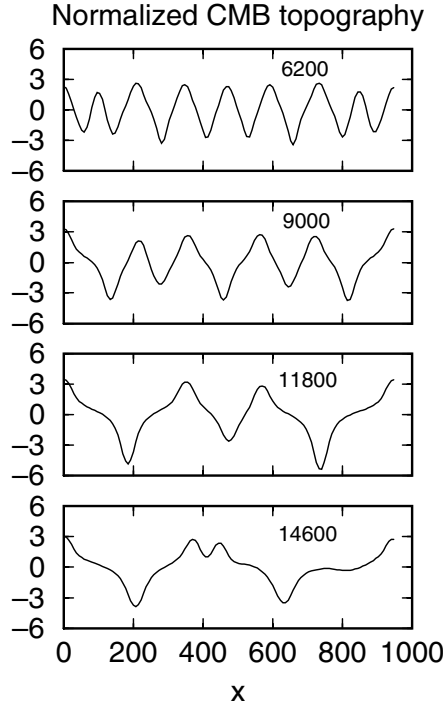


Figure 6. Topography of the CMB normalized by $\alpha T_l \delta_l$.

and 0.062 for bottom heated convection [Solomatov and Moresi, 2000].

5.7. CMB Topography

[18] The CMB topography scales with $h_0 = \alpha \Delta T_l \delta_l$ (assuming that the core density is about twice the mantle density at the CMB). Figures 4c and 6 show that the amplitude of the CMB topography is roughly $h = 2h_0$.

5.8. Onset of Small-Scale Convection

[19] In a simple case with a linear temperature gradient across the layer of thickness d , small-scale convection starts when [Stengel *et al.*, 1982]

$$d^3 = 20.9\theta^4. \quad (16)$$

This gives $d \approx 75$. In the numerical simulations, convection starts at $d \approx 60$ (Figure 2b).

5.9. Transition to Chaotic Regime

[20] The transition to chaotic regime is poorly constrained, and it depends on whether the problem is two-dimensional or three-dimensional. However, a simple criterion based on this and other studies [Dumoulin *et al.*, 1999] can be suggested: The transition occurs when the thickness of the convective layer is ~ 4 times larger than the critical one for the onset of convection.

6. Summary of Scaling Relationships in Dimensional Form

[21] A good agreement between the scaling theory for stagnant lid convection and numerical simulations of this particular problem implies that we can use these scaling laws in a broader parameter range. The basic scaling relationships for small-scale convection described with the viscosity law (5) in the D'' layer can be summarized in dimensional form as follows:

[22] For small-scale convection to develop before the thermal boundary layer becomes unstable as a whole, the viscosity contrast across the thermal boundary layer must satisfy the condition (note, however, that this is only approximately valid for Arrhenius viscosity):

$$\Delta \eta_{\text{cmb}} = \exp \frac{Q \Delta T_{\text{cmb}}}{RT_m T_c} > 10^4. \quad (17)$$

[23] Once this condition is satisfied, small-scale convection starts when the thickness of the thermal boundary layer exceeds the critical one determined by the following criterion:

$$d_{\text{cr}}^3 = 20.9 \frac{\kappa \eta_c}{\alpha \rho g \Delta T_{\text{cmb}}} \theta^4. \quad (18)$$

[24] The temperature drops in the upper and lower boundary layers are

$$\Delta T_u = T_i - T_L \approx 2.6\gamma^{-1}, \quad (19)$$

$$\Delta T_l = T_c - T_i \approx 1.1\gamma^{-1}. \quad (20)$$

[25] The amplitude of lateral temperature variations is

$$\Delta T_{\text{lat}} \approx 1.9\gamma^{-1}. \quad (21)$$

[26] The amplitude of lateral variations in the thickness of the convective layer is

$$\Delta d \approx 0.08d. \quad (22)$$

[27] The heat flux at the CMB is

$$F = 0.5k\gamma^{-4/3} \left(\frac{\alpha \rho g}{\kappa \eta_c} \right)^{1/3}. \quad (23)$$

[28] The thickness of the convective region is

$$d = \frac{Ft}{\rho c_p (T_i - T_m)}, \quad (24)$$

where t is the time elapsed from the beginning of bottom heating. Although (24) is valid for $d \gg d_{\text{cr}}$, the deviation from the exact solution is only $\sim 20\%$ even near the onset of convection (Figure 2b).

[29] The flow velocity in the convective region is

$$u = 0.05\kappa d \gamma^{-2/3} \left(\frac{\alpha \rho g}{\kappa \eta_c} \right)^{2/3}. \quad (25)$$

[30] The temperature distribution in the conductive region is

$$T = T_m + (T_L - T_m) \exp \left[-\frac{d}{\kappa} (z - dt) \right]. \quad (26)$$

[31] The width of the conductive region is

$$\delta_L = 2.3 \frac{k \Delta T_{\text{cmb}} (1 - 1.1\theta^{-1})}{F}. \quad (27)$$

[32] The thicknesses of the upper and lower boundary layers are

$$\delta_u = \frac{k \Delta T_u}{F}, \quad (28)$$

$$\delta_l = \frac{k \Delta T_l}{F}. \quad (29)$$

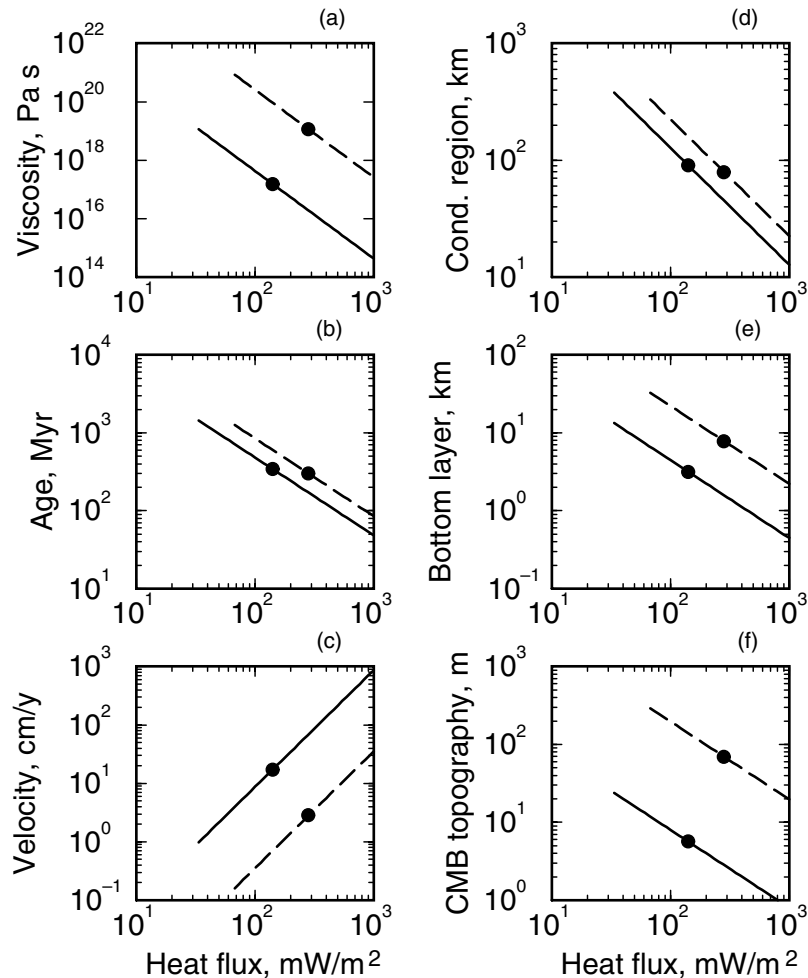


Figure 7. Various convective parameters as a function of the heat flux at the CMB: (a) the viscosity at the CMB, (b) the time it takes for the convective boundary to reach 250-km height above the CMB, (c) the flow velocity, (d) the width of the conductive region on top of the convective layer, (e) the thickness of the bottom thermal boundary layer, and (f) the magnitude of topographic undulations. The beginning of the curves corresponds to the onset of small-scale convection. The solid circle separates quasi-steady state from chaotic regime. The solid curve corresponds to $T_c = 3500$ K and $Q = 1500$ kJ mol $^{-1}$. The dashed curve corresponds to $T_c = 4500$ K and $Q = 500$ kJ mol $^{-1}$.

[33] The amplitude of the CMB topography is

$$h = 2\alpha\Delta T_1\delta_1. \quad (30)$$

Extrapolation to non-Newtonian viscosity convection is straightforward; however, the results are usually very similar [Solomatov and Moresi, 2000].

7. Physical Parameters of the D'' Layer

[34] To apply nondimensional scaling laws to the D'' layer, we need to choose the physical parameters of the D'' layer. One of the most critical parameters, the activation enthalpy for viscous creep, was discussed earlier. The prefactor in the viscosity function will be used as a free parameter. Other physical parameters are chosen as follows: $k = 6$ mW m $^{-2}$ [Hofmeister, 1999], $c_p = 1200$ kJ kg $^{-1}$ K $^{-1}$, $\rho = 5500$ kg m $^{-3}$, $g = 10.5$ m s $^{-2}$ [Anderson, 1989], $\kappa = k/\rho c_p = 9.1 \times 10^{-7}$ m 2 s $^{-1}$, and $\alpha = 1.2 \times 10^{-5}$ K $^{-1}$ [Chopelas, 1996; Gillet et al., 1996].

[35] The heat flux F_c from the core is probably larger than the adiabatic heat flux from the core which is ~ 30 mW m $^{-2}$

[Stevenson, 1981] (for the parameters assumed in our model). This is comparable with the heat flux associated with plumes [Davies, 1988; Sleep, 1990]. The heat flux from the core can probably be as high as 100 mW m $^{-2}$, which is one third of the total heat loss from the planet, which is $\sim 4.4 \times 10^{13}$ W [Pollack et al., 1993]. This value would still be consistent with the constraints on the radiogenic heating in the crust and the mantle [O'Nions et al., 1979] and on the secular cooling of the planet [Abbot et al., 1994]. For example, this value would explain the high total heat flux compared to the heating rate due to radioactive isotopes. In the past, the explanation of the surface heat flux involved such factors as a higher than chondritic concentration of radioactive elements, layering, and variable viscosity [Turcotte, 1980; McKenzie and Richter, 1981; Stevenson et al., 1983; Christensen, 1985; Solomatov, 2001]. Therefore a range between 30 and 100 mW m $^{-2}$ will be assumed.

[36] The temperature at the core-mantle boundary is likely to be between 3500 and 4500 K [Williams, 1998; Boehler, 2000]. The mantle temperature is probably close to an adiabat, although slightly superadiabatic (in case of partial mantle layering) or subadiabatic temperatures are possible (if cold slabs accumulate at

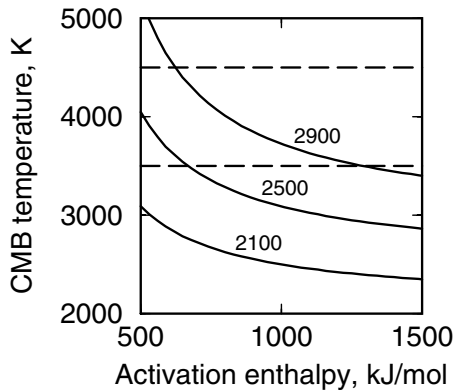


Figure 8. A graphic representation of equation (17). The curves $T_c(Q)$ show the core-mantle boundary temperature at which the viscosity contrast across the thermal boundary layer is $\Delta\eta_{\text{cmb}} = 10^4$. Small-scale convection can occur in the region above the curve. The three different curves correspond to three values of the temperature T_m at the base of the mantle (2100, 2500, and 2900 K). The dashed lines show the likely range of T_c .

the bottom of the mantle). However, the results are not very sensitive to T_m with most of the parameters being independent of T_m . We will assume $T_m = 2500$ K.

8. Results and Discussion

8.1. Estimates for Small-Scale Convection in the D'' Layer

[37] The parameters of small-scale convection are as follows. The viscosity at the CMB is $\eta_c = 10^{18} - 10^{22}$ Pa s, the convective velocity is $u = 0.1 - 10$ cm y^{-1} , the thickness of the conductive region on top of the convective region is $\delta_L = 100 - 300$ km, the thickness of the thermal boundary layer at the bottom of convective layer is $\delta_T = 3 - 30$ km, the topography of the CMB due to small-scale convection is $h = 10 - 300$ m, and the temperature variations in the convective region is $T_1 = 100 - 400$ K.

[38] The results for two end-member cases are shown in Figure 7. Figure 8 shows the parameter range where the condition (17) for the existence of small-scale convection is satisfied.

8.2. D'' Discontinuity

[39] Any theory of the D'' layer must explain the seismic velocity increase across the D'' discontinuity. In our model, chemical homogenization within the convective layer can make the convective region chemically distinct from the mantle above. This implies that convective boundary is also a chemical boundary. There is no lack of sources of chemical heterogeneity at the bottom of the mantle: chemical reactions at the CMB, subducted slabs, and partial melting and differentiation either in an early magma ocean or later during planetary evolution [Knittle and Jeanloz, 1991; Wysession et al., 1998; Tackley, 1998; Morse, 2000]. A convective/chemical boundary can be extremely sharp. This is consistent with observations which suggest that the width of the D'' discontinuity is < 50 km and could be < 8 km in some regions [Wysession et al., 1998].

[40] The observed variations in the thickness of the D'' layer, from 130 km [Vidale and Benz, 1993] to 450 km [Kendall and Shearer, 1994], can be interpreted as variations in the age of the discontinuity (e.g., since the last episode of large-scale instability) or lateral variation in the heat flux (e.g., due to lateral variations in the viscosity by a factor of 70).

[41] The intermittent appearance of the D'' discontinuity [Wysession et al., 1998] can be related to absence or presence of convection. In some regions the thermal boundary layer

might be still too thin, and convection has not started yet. In other regions the viscosity might be too high. Chemical stratification can also suppress convection in some places and not in others.

[42] An alternative explanation for the D'' discontinuity is a phase transformation [Nataf and Huard, 1993; Sidorin et al., 1999]. However, no evidence of phase transformations in the lower mantle has been found yet [Kesson et al., 1998; Serghiou et al., 1998].

8.3. Ultralow-Velocity Zone

[43] Can small-scale convection be related to the formation of the ultralow-velocity zone (ULVZ) at the base of the mantle? Seismic data indicate that it has a thickness of 5–40 km and P and S wave velocity reductions of the order of 5–30%, suggesting a possible partial melting [Garnero and Helmberger, 1995; Mori and Helmberger, 1995; Williams and Garnero, 1996; Revenaugh and Meyer, 1997; Vidale and Hedlin, 1998; Wen and Helmberger, 1998].

[44] The thickness of ULVZ is surprisingly similar to the thickness $\delta_L = 3 - 30$ km of the thermal boundary layer at the bottom of the convective region. However, the observed reduction in seismic velocities cannot be caused by temperature variations of only T_1 70–370 K and require other factors such as partial melting. Any melt generated in the D'' layer is likely to be denser than the solid matrix and would accumulate at the bottom of the D'' layer [Knittle, 1998].

[45] The intermittent appearance of the ULVZ suggests that in some regions this layer is either absent or its thickness is smaller than a few kilometers. This can partially be attributed to lateral variations in the heat flux. However, dynamics and differentiation of a partially molten thermal boundary layer is likely to play a more significant role. Also, the ULVZ might be due to factors unrelated to small-scale convection. For example, it can be formed on the other side of the core-mantle boundary as a result of accumulation of silicate sediments during solidification of the Earth's core [Buffett et al., 2000].

8.4. Lateral Temperature Variations

[46] The length scale of lateral temperature variations is of the order of the thickness of the convective layer. This is consistent with seismic data provided that the convective layer approximately coincides with the D'' layer.

[47] The amplitude of lateral temperature variations is 130–640 K with the largest amplitude obtained for the smallest $Q = 500$ kJ mol^{-1} and highest $T_c = 4500$ K. This can account for up to $\pm 3\%$ shear velocity variations [Duffy and Ahrens, 1992; Wysession et al., 1992; Wang and Weidner, 1996], although much smaller values can be obtained using Yuen et al.'s [1993] scaling. This is only marginally consistent with the observed seismic velocity variations [Weber, 1993; Lay et al., 1997; Liu et al., 1998; Castle et al., 2000]. Other factors such as chemical heterogeneities and anisotropy can be more important for seismic velocity variations. Chemical heterogeneities are likely to be present at the bottom of the convective mantle [Christensen, 1984; Davies and Gurnis, 1986; Hansen and Yuen, 1988; Kellogg, 1997; Tackley, 1998]. Since small-scale convection in the D'' layer is probably not chaotic (Figure 7), lateral mixing is not very efficient [Kellogg, 1992; Schmalz and Hansen, 1994; Ferrachat and Ricard, 1998]. It is conceivable that mixing within the D'' layer occurs mainly on length scales comparable with the thickness of the convective layer (200–300 km) and the D'' layer remains highly heterogeneous on larger scales. The anisotropy of the D'' layer [Lay et al., 1998b; Kendall and Silver, 1996; Matzel et al., 1996; Garnero and Lay, 1997] can be due to redistribution and alignment of partial melt by small-scale convection or development of lattice preferred orientation in magnesiowüstite [Wentzovitch et al., 1998].

8.5. D'' Topography

[48] The amplitude of the topography of the convection boundary is about ± 20 km for the 250-km-thick convective layer and ± 10 –35 km for the 130- to 450-km-thick layer. This is the region with the largest variations in temperature (and composition if the convective boundary is also a chemical boundary). Therefore the largest lateral variations in seismic velocities are expected in this 20- to 70-km-thick region, near the D'' discontinuity. This is in agreement with seismic data [Lay *et al.*, 1997].

8.6. CMB Topography

[49] The topography of the CMB ± 10 –400 m is consistent with seismic constraints indicating that it is less than several hundred meters thick [Shearer *et al.*, 1998].

8.7. Low-Velocity Gradients Above the D'' Discontinuity

[50] The thickness of the conductive region (130–380 km) is consistent with the thickness of the low-velocity gradient region above the D'' discontinuity (~ 300 km). The temperature drop $\Delta T_{\text{cmb}} - 3.7\gamma^{-1} = 500$ –1500 K in this region is large enough to explain $\sim 1\%$ reduction in shear wave velocities over the 300-km depth range [Wysession *et al.*, 1998].

8.8. Viscosity

[51] The viscosity at the core-mantle boundary is very similar to the viscosity in the asthenosphere which ranges from 10^{18} to 10^{20} Pa s [Rydelecks and Sacks, 1990; Sigmundsson, 1991; Zandt and Carrigan, 1993; Fjeldskaar, 1994; Kaufmann and Wolf, 1996; Pollitz *et al.*, 1998]. Application of stagnant lid convection theory to small-scale convection in the asthenosphere gives similar estimates [Davaille and Jaupart, 1994; Doin *et al.*, 1997; Dumoulin *et al.*, 1999; Solomatov and Moresi, 2000]. This is consistent with the idea that the temperature in both regions is close to solidus provided the mantle viscosity is nearly constant along solidus.

[52] For small-scale convection to occur, the viscosity of the lower mantle must be at least 10^4 times higher than the viscosity at the core-mantle boundary. This implies that mantle viscosity is at least 10^{22} – 10^{26} Pa s. This is consistent with the estimates of the viscosity for the lower mantle, 10^{22} – 10^{24} Pa s [King, 1995; Čadek and Fleitout, 1999; Forte and Mitrovica, 2001].

8.9. Instability of the D'' Layer

[53] In our numerical example the D'' layer has been continuously growing since 0.3–1.3 Gyr ago. Eventually, it would become unstable [Christensen, 1984; Olson *et al.*, 1987; Thompson and Tackley, 1998]. The instability of this layer would produce plumes with ~ 1000 K temperature contrast, while the temperature contrast in the plumes is unlikely to be more than 300 K [Watson and McKenzie, 1991]. A chemical boundary layer seems to be necessary to prevent plumes with large temperature contrasts [Farnetani, 1997]. In our model the entire convective layer can be such chemical boundary layer.

9. Conclusion

[54] Temperature and viscosity contrasts in the thermal boundary layer at the base of the mantle can be high enough for convective instability to develop first in the lower part of the thermal boundary layer before the thermal boundary layer as a whole becomes unstable. Such small-scale convection can be related to the origin of lateral heterogeneities and anisotropy in the D'' layer, the ULVZ, and the low-velocity gradients above the D'' discontinuity. It can also enhance chemical mixing within the convective region and generate a chemical boundary which would coincide with the convection boundary. This can be one of the possible origins of the D'' discontinuity. Such compositional layering might also help to reduce the temperature contrasts in

the plumes which would eventually form as a result of instabilities of the D'' layer as a whole. The small-scale convection model gives reasonable estimates for various parameters of the D'' layer including the topography of the CMB, the topography of the D'' discontinuity, and the viscosity at the base of the mantle. Lateral temperature variations due to small-scale convection are marginally consistent with the amplitude of lateral seismic velocity variations. However, the latter might be easier to explain by other factors such as topography of the convection boundary, lateral chemical variations, and anisotropy. The large seismic velocity drop in the ULVZ cannot be explained by thermal effects alone and may require melting, which is preferred by various authors. Further understanding of the structure and dynamics of the D'' layer requires investigation of melting, differentiation, and chemical mixing in the D'' layer. It would also be important to understand the dynamics of plume formation and the interaction between the small-scale processes at the base of the mantle and global mantle dynamics. Finally, we need to understand what role small-scale convection and large-scale instabilities of the convective layer play in the thermal evolution of the Earth and other terrestrial planets and how these affect tectonics, volcanism, and magnetism of the terrestrial planets.

[55] **Acknowledgments.** The authors thank Thorne Lay and Peter van Keken for thoughtful and constructive reviews. V.S. was supported by NASA and Alfred P. Sloan Foundation. L.M. was partly supported by the Australian Geodynamics Cooperative Research Centre; this work is published with the permission of the director, AGCRC.

References

- Abbot, D., L. Burgess, J. Longhi, and W. H. F. Smith, An empirical thermal history of the Earth's upper mantle, *J. Geophys. Res.*, *99*, 13,835–13,850, 1994.
- Anderson, D. L., *Theory of the Earth*, Blackwell Sci., Malden, Mass., 1989.
- Boehler, R., High-pressure experiments and the phase diagram of lower mantle and core materials, *Rev. Geophys.*, *38*, 221–245, 2000.
- Buffett, B. A., E. J. Garnero, and R. Jeanloz, Sediments at the top of Earth's core, *Science*, *290*, 1338–1342, 2000.
- Čadek, O., and L. Fleitout, A global geoid model with imposed velocities and partial layering, *J. Geophys. Res.*, *104*, 29,055–29,075, 1999.
- Castle, J. C., K. C. Creager, J. P. Winchester, and R. D. van der Hilst, Shear wave speeds at the base of the mantle, *J. Geophys. Res.*, *105*, 21,543–21,557, 2000.
- Chopelas, A., Thermal expansivity of lower mantle phases MgO and MgSiO₃ perovskite at high pressure derived from vibrational spectroscopy, *Phys. Earth Planet. Inter.*, *98*, 3–15, 1996.
- Christensen, U., Instability of a hot boundary layer and initiation of thermochemical plumes, *Ann. Geophys.*, *2*, 311–320, 1984.
- Christensen, U., Thermal evolution models of the Earth, *J. Geophys. Res.*, *90*, 2995–3007, 1985.
- Davaille, A., and C. Jaupart, Transient high Rayleigh number thermal convection with large viscosity variations, *J. Fluid Mech.*, *253*, 141–166, 1993.
- Davaille, A., and C. Jaupart, Onset of thermal convection in fluids with temperature-dependent viscosity: Application to the oceanic mantle, *J. Geophys. Res.*, *99*, 19,853–19,866, 1994.
- Davies, G. F., Ocean bathymetry and mantle convection, 1, Large-scale flow and hotspots, *J. Geophys. Res.*, *9310*, 467–10,480, 1988.
- Davies, G. F., and M. Gurnis, Interaction of mantle dregs with convection—Lateral heterogeneity at the core-mantle boundary, *Geophys. Res. Lett.*, *13*, 1517–1520, 1986.
- Doin, M.-P., L. Fleitout, and U. Christensen, Mantle convection and stability of depleted and undepleted continental lithosphere, *J. Geophys. Res.*, *102*, 2771–2787, 1997.
- Duffy, T. S., and T. J. Ahrens, Sound velocities at high pressure and temperature and their geophysical implications, *J. Geophys. Res.*, *97*, 4503–4520, 1992.
- Dumoulin, C., M. P. Doin, and L. Fleitout, Heat transport in stagnant lid convection with temperature- and pressure-dependent Newtonian or non-Newtonian rheology, *J. Geophys. Res.*, *104*, 12,759–12,777, 1999.
- Farnetani, C. G., Excess temperature of mantle plumes: The role of chemical stratification across D'', *Geophys. Res. Lett.*, *24*, 1583–1586, 1997.
- Ferrachat, S., and Y. Ricard, Regular vs. chaotic mantle mixing, *Earth Planet. Sci. Lett.*, *155*, 75–86, 1998.

- Fjeldskaar, W., Viscosity and thickness of the asthenosphere detected from the Fennoscandian uplift, *Earth Planet. Sci. Lett.*, 126, 399–410, 1994.
- Forste, A. M., and J. X. Mitrovica, Deep-mantle high-viscosity flow and thermochemical structure inferred from seismic and geodynamic data, *Nature*, 410, 1049–1056, 2001.
- Fowler, A. C., Fast thermoviscous convection, *Stud. Appl. Math.*, 72, 1–34, 1985.
- Garnero, E. J., Heterogeneity of the lowermost mantle, *Annu. Rev. Earth Planet. Sci.*, 28, 509–537, 2000.
- Garnero, E. J., and D. V. Helmberger, A very slow basal layer underlying large-scale low-velocity anomalies in the lower mantle beneath the Pacific: Evidence from core phases, *Phys. Earth Planet. Inter.*, 91, 161–176, 1995.
- Garnero, E. J., and T. Lay, Lateral variations in lowermost mantle shear wave anisotropy beneath the North Pacific and Alaska, *J. Geophys. Res.*, 102, 8121–8135, 1997.
- Gillet, P., F. Guyot, and Y. Wang, Microscopic anharmonicity and equation of state of MgSiO₃-perovskite, *Geophys. Res. Lett.*, 21, 3043–3304, 1996.
- Grand, S. P., Mantle structure beneath the Americas and surrounding oceans, *J. Geophys. Res.*, 99, 11,591–11,622, 1994.
- Grand, S. P., R. D. van der Hilst, and S. Widiyantoro, Global seismic tomography: A snapshot of convection in the Earth, *GSA Today*, 7, 1–7, 1997.
- Grasset, O., and E. M. Parmentier, Thermal convection in a volumetrically heated, infinite Prandtl number fluid with strongly temperature-dependent viscosity: Implications for planetary evolution, *J. Geophys. Res.*, 103, 18,171–18,181, 1998.
- Hansen, U., and D. A. Yuen, Numerical simulations of thermal-chemical instabilities at the core-mantle boundary, *Nature*, 334, 237–240, 1988.
- Hofmeister, A. M., Mantle values of thermal conductivity and the geotherm from phonon lifetimes, *Science*, 283, 1699–1706, 1999.
- Ita, J., and R. E. Cohen, Diffusion in MgO at high pressure: Implications for lower mantle rheology, *Geophys. Res. Lett.*, 25, 1095–1098, 1998.
- Karato, S., and P. Li, Diffusion creep in perovskite: Implications for the rheology of the lower mantle, *Science*, 255, 1238–1240, 1992.
- Kaufmann, G., and D. Wolf, Deglacial land emergence and lateral upper-mantle heterogeneity in the Svalbard Archipelago, II. Extended results for high resolution load models, *Geophys. J. Int.*, 127, 125–140, 1996.
- Kellogg, L. H., Mixing in the mantle, *Annu. Rev. Earth Planet. Sci.*, 20, 365–388, 1992.
- Kellogg, L. H., Growing the Earth's D'' layer: Effect of density variations at the core-mantle boundary, *Geophys. Res. Lett.*, 24, 2749–2752, 1997.
- Kendall, J.-M., and P. M. Shearer, Lateral variations in D'' thickness from long-period shear wave data, *J. Geophys. Res.*, 99, 11,575–11,590, 1994.
- Kendall, J.-M., and P. G. Silver, Constraints from seismic anisotropy on the nature of the lowermost mantle, *Nature*, 381, 409–412, 1996.
- Kesson, S. E., J. D. Fitz Gerald, and J. M. Shelley, Mineralogy and dynamics of a pyrolite lower mantle, *Nature*, 393, 252–255, 1998.
- King, S. D., Models of mantle viscosity, in *Mineral Physics and Crystallography: A Handbook of Physical Constants*, AGU Ref. Shelf Ser., vol. 2, edited by T. J. Ahrens, pp. 227–236, AGU, Washington, D. C., 1995.
- Knittle, E., The solid-liquid partitioning of major and radiogenic elements at lower mantle pressures: Implications for the core-mantle boundary region, in *The Core-Mantle Boundary Region*, *Geodyn. Ser.*, vol. 28, edited by M. Gurnis et al., pp. 119–130, AGU, Washington, D. C., 1998.
- Knittle, E., and R. Jeanloz, Earth's core-mantle boundary: Results of experiments at high pressures and temperatures, *Science*, 251, 1438–1443, 1991.
- Lay, T., E. J. Garnero, C. J. Young, and J. B. Gaherty, Scale-lengths of shear velocity heterogeneity at the base of the mantle from S wave differential travel times, *J. Geophys. Res.*, 102, 9887–9910, 1997.
- Lay, T., E. J. Garnero, Q. Williams, L. Kellogg, and M. E. Wysession, Seismic wave anisotropy in the D'' region and its implications, in *The Core-Mantle Boundary Region*, *Geodyn. Ser.*, vol. 28, edited by M. Gurnis et al., pp. 299–318, AGU, Washington, D. C., 1998a.
- Lay, T., Q. Williams, and E. J. Garnero, The core-mantle boundary layer and deep Earth dynamics, *Nature*, 392, 461–468, 1998b.
- Li, P., S.-I. Karato, and Z. Wang, High-temperature creep in fine-grained polycrystalline CaTiO₃, an analogue material of (Mg,Fe)SiO₃ perovskite, *Phys. Earth Planet. Inter.*, 95, 19–36, 1996.
- Liu, X.-F., J. Tromp, and A. M. Dziewonski, Is there a first-order discontinuity in the lowermost mantle?, *Earth Planet. Sci. Lett.*, 160, 343–351, 1998.
- Loper, D., and T. Lay, The core-mantle boundary region, *J. Geophys. Res.*, 100, 6397–6420, 1995.
- Loper, D., and F. D. Stacey, The dynamical and thermal structure of deep mantle plumes, *Phys. Earth Planet. Inter.*, 33, 304–317, 1983.
- Manga, M., D. Weeraratne, and S. J. S. Morris, Boundary-layer thickness and instabilities in Benard convection of a liquid with a temperature-dependent viscosity, *Phys. Fluids*, 13, 802–805, 2001.
- Matzel, E., M. K. Sen, and S. P. Grand, Evidence for anisotropy in the deep mantle beneath Alaska, *Geophys. Res. Lett.*, 23, 2417–2420, 1996.
- McKenzie, D. P., and F. M. Richter, Parameterized thermal convection in a layered region and the thermal history of the Earth, *J. Geophys. Res.*, 86, 11,667–11,680, 1981.
- Meade, C., P. G. Silver, and S. Kaneshima, Laboratory and seismological observations of lower mantle isotropy, *Geophys. Res. Lett.*, 22, 1293–1296, 1995.
- Montague, N. L., and L. H. Kellogg, Numerical models of a dense layer at the base of the mantle and implications for the geodynamics of D'', *J. Geophys. Res.*, 105, 11,101–11,114, 2000.
- Mori, J., and D. V. Helmberger, Localized boundary layer below the mid-Pacific velocity anomaly identified from a PcP precursor, *J. Geophys. Res.*, 100, 20,359–20,365, 1995.
- Morse, S. A., A double magmatic heat pump at the core-mantle boundary, *Am. Mineral.*, 85, 1589–1594, 2000.
- Nataf, H. C., and S. Huard, Seismic discontinuity at the top of D'': A world-wide feature?, *Geophys. Res. Lett.*, 20, 2371–2374, 1993.
- O'Nions, R. K., N. M. Evensen, and P. J. Hamilton, Geochemical modeling of mantle differentiation and crustal growth, *J. Geophys. Res.*, 84, 6091–6101, 1979.
- Olson, P., G. Schubert, and C. Anderson, Plume formation in the D''-layer and the roughness of the core-mantle boundary, *Nature*, 327, 409–413, 1987.
- Pollack, H. N., S. J. Hurter, and J. R. Johnson, Heat flow from the Earth's interior: Analysis of the global data set, *Rev. Geophys.*, 31, 267–280, 1993.
- Pollitz, F. F., R. Bürgmann, and B. Romanowicz, Viscosity of oceanic asthenosphere inferred from remote triggering of earthquakes, *Science*, 280, 1245–1249, 1998.
- Revenaugh, J. S., and R. Meyer, Seismic evidence of partial melt within a possibly ubiquitous low velocity layer at the base of the mantle, *Science*, 277, 670–673, 1997.
- Ribe, N. M., and D. P. de Valpine, The global hotspot distribution and instability of D'', *Geophys. Res. Lett.*, 21, 1507–1510, 1994.
- Rydelecks, P. A., and I. S. Sacks, Asthenospheric viscosity and stress diffusion: A mechanism to explain correlated earthquakes and surface deformation in NE Japan, *Geophys. J. Int.*, 100, 39–58, 1990.
- Schmalz, J., and U. Hansen, Mixing the Earth's mantle by thermal convection: A scale dependent phenomenon, *Geophys. Res. Lett.*, 21, 987–990, 1994.
- Serghiou, G., A. Zerr, and R. Boehler, (Mg,Fe)SiO₃-perovskite stability under lower mantle conditions, *Science*, 280, 2093–2095, 1998.
- Shearer, P. M., M. A. H. Hedlin, and P. S. Earle, PKP and PKKP precursor observations: Implications for the small-scale structure of the deep mantle and core, in *The Core-Mantle Boundary Region*, *Geodyn. Ser.*, vol. 28, edited by M. Gurnis et al., pp. 37–55, AGU, Washington, D. C., 1998.
- Sidorin, I., M. Gurnis, and D. V. Helmberger, Evidence for a ubiquitous seismic discontinuity at the base of the mantle, *Science*, 286, 1326–1331, 1999.
- Sigmundsson, F., Post-glacial rebound and asthenosphere viscosity in Iceland, *Geophys. Res. Lett.*, 18, 1131–1134, 1991.
- Sleep, N. H., Hotspots and mantle plumes: Some phenomenology, *J. Geophys. Res.*, 95, 6715–6736, 1990.
- Solomatov, V. S., Scaling of temperature- and stress-dependent viscosity convection, *Phys. Fluids*, 7, 266–274, 1995.
- Solomatov, V. S., Grain-size dependent viscosity convection and the thermal evolution of the Earth, *Earth Planet. Sci. Lett.*, 191, 203–212, 2001.
- Solomatov, V. S., and L.-N. Moresi, Scaling of time-dependent stagnant lid convection: Application to small-scale convection on the Earth and other terrestrial planets, *J. Geophys. Res.*, 105, 21,795–21,818, 2000.
- Stengel, K. C., D. C. Oliver, and J. R. Booker, Onset of convection in a variable viscosity fluid, *J. Fluid. Mech.*, 120, 411–431, 1982.
- Stevenson, D. J., Models of the Earth's core, *Science*, 214, 611–619, 1981.
- Stevenson, D. J., T. Spohn, and G. Schubert, Magnetism and thermal evolution of the terrestrial planets, *Icarus*, 54, 466–489, 1983.
- Tackley, P. J., Three-dimensional simulations of mantle convection with thermo-chemical basal boundary layer: D'', in *The Core-Mantle Boundary Region*, *Geodyn. Ser.*, vol. 28, edited by M. Gurnis et al., pp. 231–253, AGU, Washington, D. C., 1998.
- Thompson, P. E., and P. J. Tackley, Generation of mega-plumes from the core-mantle boundary in a compressible mantle with temperature-dependent viscosity, *Geophys. Res. Lett.*, 25, 1999–2002, 1998.
- Trompert, R. A., and U. Hansen, On the Rayleigh number dependence of convection with a strongly temperature-dependent viscosity, *Phys. Fluids*, 10, 351–360, 1998.
- Turcotte, D. L., On the thermal evolution of the Earth, *Earth Planet. Sci. Lett.*, 48, 53–58, 1980.

- van der Hilst, H. R., S. Widiyantoro, and E. R. Engdahl, Evidence for deep mantle circulation from global tomography, *Nature*, 386, 578–584, 1997.
- Vidale, J. E., and H. M. Benz, Seismological mapping of fine structure near the base of the Earth's mantle, *Nature*, 361, 529–532, 1993.
- Vidale, J. E., and A. H. Hedlin, Evidence for partial melt at the core-mantle boundary north of Tonga from the strong scattering of seismic waves, *Nature*, 391, 682–685, 1998.
- Wang, Y., and D. J. Weidner, $(\partial\mu/\partial T)_P$ of the lower mantle, *Pure Appl. Geophys.*, 146, 533–549, 1996.
- Wang, Z.-C., C. Dupas-Bruzek, and S. Karato, High temperature creep of an orthorhombic perovskite— YAlO_3 , *Phys. Earth Planet. Inter.*, 110, 51–69, 1999.
- Watson, S., and D. P. McKenzie, Melt generation by plumes: A study of Hawaiian volcanism, *J. Petrol.*, 12, 501–537, 1991.
- Weber, M., P and S wave reflections from anomalies in the lowermost mantle, *Geophys. J. Int.*, 115, 183–210, 1993.
- Wen, L., and D. V. Helmberger, Ultra-low velocity zones near the core-mantle boundary from broadband PKP precursors, *Science*, 279, 1701–1703, 1998.
- Wentzcovitch, R. M., B. B. Karki, S. Karato, and C. R. S. Da Silva, High pressure elastic anisotropy of MgSiO_3 perovskite and geophysical implications, *Earth Planet. Sci. Lett.*, 164, 371–378, 1998.
- Williams, Q., The temperature contrast across D'' , in *The Core-Mantle Boundary Region*, *Geodyn. Ser.*, vol. 28, edited by M. Gurnis et al., pp. 73–81, AGU, Washington, D. C., 1998.
- Williams, Q., and E. J. Garnero, Seismic evidence for partial melt at the base of Earth's mantle, *Science*, 273, 1528–1530, 1996.
- Wysession, M. E., E. A. Okal, and C. R. Bina, The structure of the core-mantle boundary from diffracted waves, *J. Geophys. Res.*, 97, 8749–8764, 1992.
- Wysession, M. E., T. Lay, J. Revenaugh, Q. Williams, E. J. Garnero, R. Jeanloz, and L. H. Kellogg, The D'' discontinuity and its implications, in *The Core-Mantle Boundary Region*, *Geodyn. Ser.*, vol. 28, edited by M. Gurnis et al., pp. 273–297, AGU, Washington, D. C., 1998.
- Yamazaki, D., and S.-I. Karato, Some mineral physics constraints on the rheology and geothermal structure of Earth's lower mantle, *Am. Mineral.*, 86, 385–391, 2001.
- Young, C. J., and T. Lay, The core-mantle boundary, *Annu. Rev. Earth Planet. Sci.*, 15, 25–46, 1987.
- Yuen, D. A., and W. R. Peltier, Mantle plumes and the thermal stability of the D'' layer, *Geophys. Res. Lett.*, 7, 625–628, 1980.
- Yuen, D. A., O. Cadec, A. Chopelas, and C. Matyska, Geophysical inferences of thermal-chemical structures in the lower mantle, *Geophys. Res. Lett.*, 20, 899–902, 1993.
- Zandt, G., and C. R. Carrigan, Small-scale convection instability and upper mantle viscosity under California, *Science*, 261, 460–463, 1993.

L.-N. Moresi, Australian Geodynamics Cooperative Research Centre, CSIRO Exploration and Mining, 39 Fairway, Nedlands 6009, Western Australia, Australia. (louis@ned.dem.csiro.au)

V. S. Solomatov, Department of Physics, New Mexico State University, Las Cruces, NM 88003, USA. (slava@nmsu.edu)